



Cite this: *Nanoscale*, 2019, **11**, 19291

Received 18th July 2019,
 Accepted 8th September 2019

DOI: 10.1039/c9nr06101k

rsc.li/nanoscale

Plasmonic bimetallic nanodisk arrays for DNA conformation sensing†

Thanh Thi Van Nguyen,^a Xiaoji Xie,^b Jiahui Xu,^b Yiming Wu,^b Minghui Hong^c and Xiaogang Liu^{b,d,e}

The integration of large-scale 2D bimetallic Ag/Au nanodisk arrays with gold nanoparticles is developed for sensing DNA conformation with the assistance of 3D finite-difference time-domain simulation. The optimized system comprising Ag/Au nanodisk arrays and gold nanoparticles offers a more than 6-fold enhancement in surface plasmon resonance shift, enabling the feasibility for sensitive DNA detection with a detection limit down to 100 femtomolar. Importantly, owing to the distance-dependent nature of the surface plasmon signal, sensitive differentiation of DNA conformations can be achieved with a conventional optical measurement. This platform could provide new exciting capabilities for a reliable, reproducible, and label-free assay analysis for investigating the conformations of DNA and other biological molecules.

Introduction

DNA molecules can form a variety of structures including the bulge, heparin, triplex, G-quadruplex and the well-known double-helical structure. These DNA conformations play critical roles in gene duplication and expression in many biological processes. An improper modulation of DNA conformations often leads to serious diseases such as Parkinson's, Alzheimer's, and diabetes.^{1,2} Therefore, understanding the DNA conformations is essential for disease diagnostics and

therapeutics. A vast number of approaches are available for the differentiation of DNA conformations, including those based on X-ray crystallography, nuclear magnetic resonance, circular dichroism, and quartz crystal microbalance.^{3–7} Although these methods can provide valuable structural information, they are rather complicated, costly and time-consuming.

Alternatively, plasmonic biosensors based on metallic nanostructures offer a facile, real-time technique for biomolecule detection while enabling parallel monitoring of multiple species, owing to their surface plasmon resonance (SPR) characteristics.^{8–32} Despite the advances in biomolecular sensing, traditional SPR-based sensors often suffer from low throughput. The sensitivity and selectivity of typical SPR-based sensors still fall short of expectations for clinical use.^{33–43} Furthermore, DNA conformation sensing using conventional SPR-based sensors remains a formidable challenge.

Herein, we present a rational design and fabrication of large-scale gold nanoparticle-integrated 2D bimetallic Ag/Au nanodisk arrays for highly sensitive DNA conformation studies by strong plasmonic coupling between the nanodisk array and gold nanoparticles (Fig. 1a). In our design, we firstly adopt a versatile nanofabrication technique, based on laser interference lithography (LIL), to fabricate and optimize 2D plasmonic Ag/Au bimetallic layer nanodisk arrays on quartz or silicon substrates over a large area through a standard lithography process (Fig. 1b and Fig. S1†).^{44–48} This long-range ordered plasmonic array provides a new opportunity to allow for a reproducible, high-throughput and label-free assay. Subsequently, a DNA sensor with a sandwich structure is developed by integrating the as-prepared 2D Ag/Au nanodisk array with DNA-modified gold nanoparticles. Strong coupling between the DNA-modified gold nanoparticles and nanodisk array significantly increases the localized plasmonic response, thus improving detection sensitivity. This nanoarray-based sensor also enables the differentiation of various DNA configurations such as bulge and G-quadruplex.

^aAdvanced Materials for Micro- and Nano-Systems Programme, Singapore-MIT Alliance, 117576, Singapore

^bDepartment of Chemistry, National University of Singapore, 3 Science Drive 3, 117543, Singapore. E-mail: chmlx@nus.edu.sg

^cDepartment of Electrical and Computer Engineering, National University of Singapore, 117576, Singapore

^dThe N.1 Institute for Health, National University of Singapore, 28 Medical Dr. #05-COR, 117456, Singapore

^eJoint School of National University of Singapore and Tianjin University, International Campus of Tianjin University, Fuzhou, 350207, P. R. China

†Electronic supplementary information (ESI) available. See DOI: 10.1039/c9nr06101k

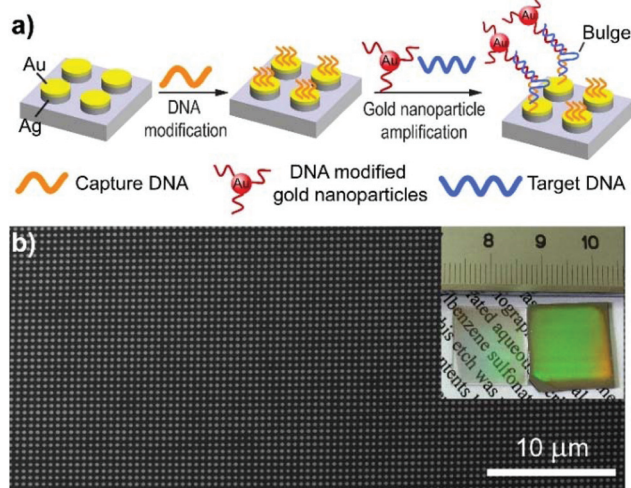


Fig. 1 (a) Schematic design of the Ag/Au nanodisk array-based sensor for DNA conformation detection through DNA-modified gold nanoparticle amplification. (b) SEM image of the as-prepared Ag/Au nanodisk array. The inset is a typical photo image of the large-scale bimetallic nanodisk array on a quartz (left) substrate and a silicon (right) substrate.

Results and discussion

Fig. 2a shows a typical scanning electron microscopy image of the as-prepared Ag/Au (20/10 nm) nanodisk array. Notably, the integration of Au with Ag benefits from both the chemical stability of Au and the sharper plasmon resonance of Ag, thus offering considerable advantages over single-metallic nanodisk arrays (Fig. S2†). As an added benefit, the well-known Au–S chemistry lays the foundation for surface functionalization. As shown in Fig. 2a, the period, diameter and total thickness of the resulting nanodisk arrays are ~ 520 nm, ~ 330 nm, and ~ 30 nm, respectively. To obtain a nanodisk array structure with optimized SPR properties, the thickness of the Ag and Au layers was varied: 10/20 nm, 15/15 nm and 20/10 nm (Ag/Au), respectively. The refractive index sensitivity study of the resulting nanoarrays reveals that a thicker Ag layer offers better sensitivity, which is attributed to the longer electromagnetic field decay length of the Ag layer compared to the Au layer (Fig. 2b).⁴⁹ However, the thickness of the Au layer in bimetallic

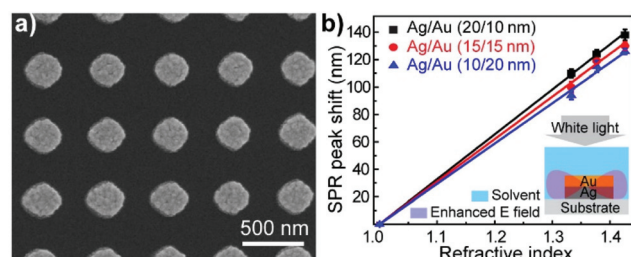


Fig. 2 (a) SEM image of the as-prepared Ag/Au nanodisk array. (b) Dependence of the SPR peak shift on the refractive index of the surrounding solvent for the as-prepared nanodisk arrays with different Ag and Au layer thicknesses.

nanodisks has to be no less than 10 nm so that there could be sufficient space for DNA functionalization. The refractive index sensitivity reaches as high as 328 nm RIU^{-1} for the Ag/Au (20/10 nm) nanodisk array. Furthermore, finite-difference time-domain (FDTD) simulation confirms that a thicker Ag layer can give rise to a more intense electromagnetic field in both transverse and longitudinal cross-sections (Fig. S3†).

In our sensing experiment, the Ag/Au (20/10 nm) nanodisk array was firstly modified with thiol-functionalized DNA^{20–32} and then hybridized with DNA-modified gold nanoparticles in the presence of an entirely complementary target DNA (t1, 24 bases) to form a sandwich structure, as shown in Fig. 3a. After the attachment of gold nanoparticles, an incremental SPR shift and peak broadening ($\Delta\text{FWHM} = 126 \text{ nm}$) were observed (Fig. 3b and Fig. S4†). The maximally increased red-shift ($\Delta\lambda_{\text{max}}$) of the SPR peak could be up to 650% for the Ag/Au (20/10 nm) nanoarray, which is higher than that achievable by previously reported single-layer nanostructures.^{37–43} In principle, this enhanced shift of the SPR peak could be attributed to two main reasons: (1) the increase of the local refractive index and (2) near-field plasmonic interactions between Ag/Au nanodisks and gold nanoparticles. To gain insight into the mechanisms responsible for the enhancement of the SPR, we employed FDTD simulation to investigate the plasmonic coupling between the nanoarray substrate and Au nanoparticles.

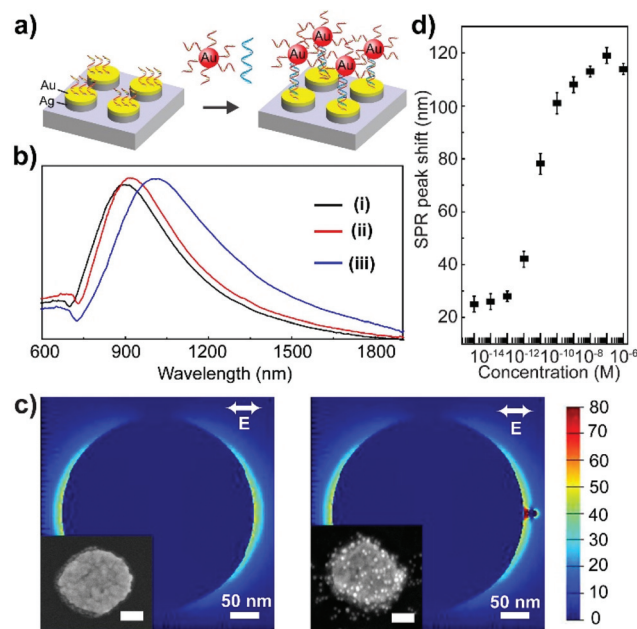


Fig. 3 Plasmonic characteristics of the Ag/Au (20/10 nm) nanodisk array enhanced by DNA-modified gold nanoparticles. (a) Schematic representation of standard sandwich DNA hybridization using DNA-modified gold nanoparticles. (b) Extinction spectra of the Ag/Au (20/10 nm) nanodisk array (i) modified with capture DNA, (ii) hybridized with linker DNA, and (iii) hybridized with linker DNA and DNA-modified gold nanoparticles. (c) FDTD simulation of the electromagnetic field of the Ag/Au (20/10 nm) nanodisk array before and after nanoparticle attachment (insets: the corresponding SEM images of the Ag/Au (20/10 nm) nanodisk array, scale bar: 100 nm). (d) SPR peak shifts at various concentrations of the target ssDNA.

On the basis of an entirely complementary target DNA with 24 bases, we assumed that the distance between the nanodisk and gold nanoparticles is 8.0 nm. The simulation results revealed that the localized electromagnetic field was significantly improved after the Au nanoparticles approached the nanoarray surface (Fig. 3c). Considering that the gold nanoparticles were attached all around the nanodisk (Fig. 3c inset), the multiplication of the plasmonic interactions from all the gold nanoparticles results in an exceedingly substantial enhancement of the SPR response of the nanodisk. These simulation results revealed that the near-field plasmonic interaction is the dominant factor for the incremental SPR shift. Taken together, these data suggest the critical role of Au nanoparticles in enhancing the SPR effect on the nanodisk substrate.

We next tested the sensitivity of our assay platform by varying the concentration of a 24-base target ssDNA (t1, 24 bases, from 1 fM to 100 nM). As shown in Fig. 3d, a lower concentration of the target DNA resulted in a smaller SPR shift due to the weak coupling effect of gold nanoparticles and the nanodisk (Fig. S5†). The nanoarray-based sensor could readily detect 1 pM target DNA with the assistance of DNA-modified gold nanoparticles. According to the Langmuir adsorption equation, the detection limit of our platform is about 100 fM (Fig. S6†).⁴²

Another essential characteristic of our sandwich-based SPR sensor is distance dependence. To study the distance-dependent plasmon property, we varied target DNA molecules with different lengths (24, 48, 72, and 96 bases) to control the distance between the gold nanoparticles and nanodisk substrate. Target DNA molecules with different lengths were first attached to the nanodisk array to verify the effect of bare DNA molecules. The SPR shift increased with the increase in the DNA length (Fig. S7†). Meanwhile, the SPR shift became almost constant when the DNA length was as long as 48 bases. Subsequently, we studied the SPR peak shift after decorating the DNA-modified gold nanoparticles in the presence of various target DNAs. The SPR peak shift increased when the DNA length increased from 24 to 48 bases after binding of gold nanoparticles (Fig. S8†). A ~ 130 nm shift was observed in the presence of 48-base target DNA when gold nanoparticles were attached. However, the SPR shift decreased sharply with further increase in the DNA length under the same conditions.

Similarly, FDTD-simulated localized electromagnetic fields also indicate the decay of the field as the distance between a gold nanoparticle and a nanodisk increases (Fig. S8†). Based on these data, we believe that the SPR shift enhancement is initially due to an increase in the refractive index attributed to the thicker DNA layer and plasmonic interactions between Ag/Au nanodisks and gold nanoparticles. Importantly, the plasmonic interactions between the nanodisks and gold nanoparticles dominate the SPR shift of the nanodisk array. For DNA strands with longer lengths, reduced electromagnetic field interactions cause a decrease in the SPR shift.

Benefiting from the high sensitivity nature of the nanodisk array-based sensor, we postulate that our platform could be used to distinguish the configurations of biomolecules. As a

proof-of-concept experiment, two double-stranded DNA strands with different configurations were chosen: a 53-base linear DNA strand (linear DNA) and a 53-base strand with one bulged structure (bulged DNA). It is worth mentioning that the 53-base bulged DNA used here contains a bulged defect with three adenine bases, which can bend double-stranded DNA (Fig. 4a).^{50,51} We then hybridized the double-stranded DNA with the DNA-modified nanodisk array and gold nanoparticles and measured the SPR shift. Inspiringly, the nanodisk array containing linear DNAs showed a smaller SPR shift (~ 98 nm) when compared with the one containing bulged DNAs (~ 118 nm) (Fig. 4b and c). This could be attributed to the short distance between the nanodisk and gold nanoparticles caused by the bending conformation of bulged DNA strands. As a result, stronger electromagnetic interactions were achieved in the presence of bulged DNAs compared to with linear DNAs. In the following set of experiments, double-stranded DNA strands with two and three bulges were com-

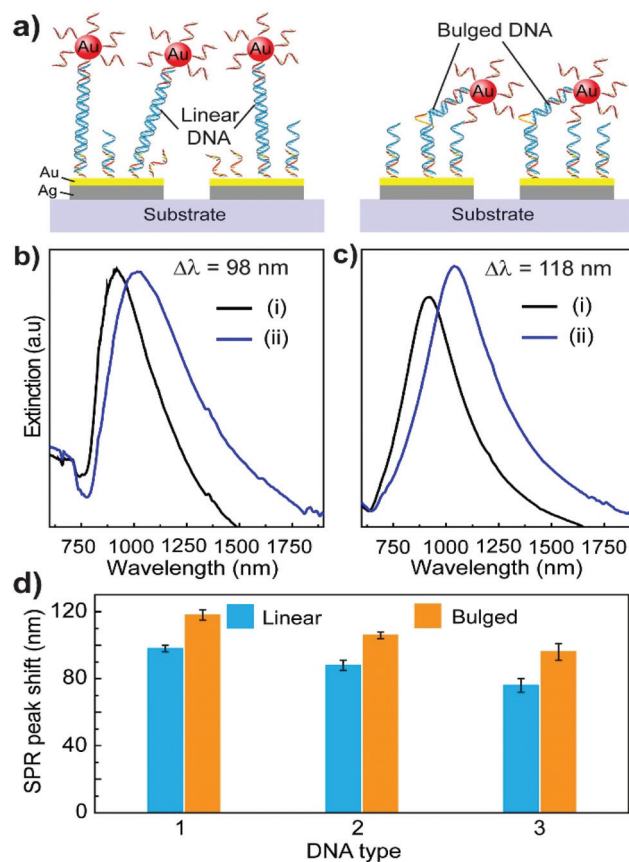


Fig. 4 (a) Schematic presentation of the linear and bulged DNA probing using the nanodisk array-based sensor with the assistance of DNA-modified gold nanoparticles. (b) and (c) Extinction spectra of the DNA-modified nanodisk array and the extinction spectra of the corresponding nanoarray hybridized with linear DNA and bulged DNA (100 nM each) in the presence of DNA-modified gold nanoparticles, respectively. (d) SPR peak shift of the nanodisk array-based sensors in the presence of DNA molecules with one, two and three bulges and their corresponding linear DNAs (100 nM each), respectively.

pared with their linear analogs using our nanodisk array sensor under identical conditions. Similarly, we can also easily distinguish the bulged DNAs from their analogs (Fig. 4d).

To demonstrate the feasibility of our platform for DNA structure differentiation, we extended our approach to probe the G-quadruplex topology. Herein, a DNA strand, which could adopt two different G-quadruplex topologies in Na⁺ and K⁺ buffers, respectively, was employed.⁵ The topology of the DNA strand in Na⁺ buffer could bring the gold nanoparticles closer to the Ag/Au nanodisk surface than that in K⁺ buffer. The procedure of the attachment of G-quadruplex topology DNAs to Ag/Au nanodisks is basically the same as that described for the linear DNAs. However, the G-quadruplex topology of DNA must be pre-formed before being attached to the nanodisk. Consequently, the DNA strand in Na⁺ buffer induced a larger SPR shift than that in K⁺ buffer upon attachment to gold nanoparticles (Fig. S9†).

Conclusions

In conclusion, we have systematically demonstrated a versatile and straightforward plasmonic enhancement platform for DNA conformation sensing that utilizes an integration of large-scale bimetallic Ag/Au nanodisk arrays and DNA-modified gold nanoparticles. A small difference in the conformation of DNA can be observed by conventional optical spectroscopy *via* DNA-modified gold nanoparticle amplification. By integrating nanofabrication with biological interactions, we introduce an alternative sensor-on-chip platform to detect conformational changes associated with biomolecules. We believe that this approach could also be extended to identify a broad range of other types of targets, including proteins, aptamer-binding small molecules, and metal ions at ultra-low concentrations.

Experimental section

Materials

400 μm thick quartz substrates were purchased from Photonik Pte Ltd, Singapore. A negative photoresist ma-N1407 was purchased from Micro resist technology, Germany. All deposition materials (Au, Ag, and Cr) were purchased from MOS Group Pte Ltd, Singapore. All DNA sequences and chemicals used for DNA experiments were purchased from Sigma-Aldrich, Singapore.

Fabrication of Ag/Au bimetallic nanodisk arrays

A large area of 2D nanodisk array was fabricated using the laser interference lithography (LIL) technique in a home-built *Lloyd's-mirror* LIL system with a 325 nm He–Cd laser. The fabrication process is shown in Fig. S1† schematically. Briefly, the negative photoresist ma-N1407 was first spin-coated on cleaned 400 μm thick quartz substrates. The photoresist-coated substrates were then baked for 90 seconds at 110 °C. In the following exposure step, the interference angle was tuned to achieve the designed parameters of the arrays. After

exposure and development to generate hole-arrays on the photoresist, less than 2 nm chromium was first deposited as the adhesion layer, followed by silver and gold film deposition by using an e-beam evaporator (EB03 BOC Edwards) on the substrate. The thickness of each metal layer was set in the e-beam evaporator system to achieve the desired thickness. A lift-off process was performed using an ma-R 404 remover.

Preparation of DNA-modified gold nanoparticles

Gold nanoparticles (~14 nm) were prepared through citrate reduction of HAuCl₄.⁵² DNA-modified gold nanoparticles were prepared according to the literature method.⁵³ Briefly, 50 μL of 3'- or 5'-terminal disulfide groups of single-stranded DNA (100 μM) was first cleaved by soaking them in a mixture of 0.1 M dithiothreitol and a phosphate buffer solution (pH = 8) for 2 hours and subsequently purified using a NAP-5 column (GE Healthcare). A solution of purified oligonucleotides (200 μL) was then added to a gold nanoparticle solution (800 μL). The resulting solution was mixed with a solution of 300 mM NaCl and 10 mM NaH₂PO₄/Na₂HPO₄ (final concentration). After 48 hours, the nanoparticle solution was centrifuged and re-dispersed in 300 mM NaCl, 10 mM PB buffer, pH = 7.

Preparation of DNA-modified Ag/Au nanodisks

Capture DNA-modified Ag/Au nanodisks were prepared by a procedure similar to gold nanoparticles. Generally, the Ag/Au nanodisks were first rinsed with deionized water and dried under ambient nitrogen gas after fabrication. Subsequently, the Ag/Au nanodisks were exposed to a solution of purified 3'- or 5'-terminal sulfide oligonucleotides and allowed to stand for 24 hours. Then, the nanodisk arrays were rinsed with deionized water to remove nonspecific DNA binding strands.

Localized surface plasmon resonance enhancement by DNA-modified gold nanoparticles

Firstly, the nanodisk arrays were modified with capture DNA (*a*), and gold nanoparticles were modified with capture DNA (*b*). The DNA-attached nanoarrays were then exposed to a solution containing 50 μL of DNA-modified gold nanoparticles and 50 μL of single-stranded target DNA (*t*). After allowing them to stand for 2 hours at room temperature, the nanodisk arrays were rinsed thoroughly with buffer solution (300 mM NaCl, 10 mM NaH₂PO₄/Na₂PO₄, pH = 7.0) before spectroscopic characterization.

For the distance-dependent study and bulged DNA configuration differentiation, the capture DNAs and target DNAs were replaced by the corresponding DNAs, as shown in the ESI.† Note that for the differentiation of bulged DNA configuration, the length of the linear DNA was kept the same as the length of the respective bulged DNA.

Detection of G-quadruplex configurations

Firstly, the nanodisk arrays were modified with capture DNA (*a2*), and gold nanoparticles were modified with capture DNA (*b2*). Note that the DNA-modified gold nanoparticles, dispersed in buffer solution (K⁺ buffer: 10 mM Tris (pH 7.0) and

100 mM KCl; Na⁺ buffer: 10 mM Tris (pH = 7.0) and 100 mM NaCl), have the desired G-quadruplex configuration. In addition, a proper buffer must be used to attach the capture DNA strands to nanodisk arrays. Subsequently, 10 μM (final concentration) G-Q strands were incubated in either K⁺ buffer or Na⁺ buffer at 90 °C for 10 minutes and then cooled down gradually to room temperature. During this step, the G-Q DNA strands that show the linear topology change to the G-quadruplex topology. DNAs with the G-quadruplex topology became the target DNAs. The capture DNA-attached nanoarrays were then exposed to a solution containing 50 μL of DNA-modified gold nanoparticles and 50 μL of 1 μM (final concentration) incubated G-Q strand solution. DNAs with the G-quadruplex topology played a role as linker DNAs in the attachment of DNA-modified gold nanoparticles to DNA-modified nanodisks. After allowing them to stand for 3 hours at room temperature, the nanodisk arrays were rinsed thoroughly with buffer solution before spectroscopic characterization.

Conflicts of interest

There are no conflicts to declare.

Acknowledgements

This study was supported by the Singapore-MIT Alliance, the Singapore Ministry of Education (MOE2017-T2-2-110), the Agency for Science, Technology and Research (A*STAR) (Grant No. A1883c0011), and the National Research Foundation, Prime Minister's Office, Singapore under its Competitive Research Program (Award No. NRF-CRP15-2015-03) and the NRF Investigatorship Programme (Award No. NRF-NRFI05-2019-0003).

Notes and references

- 1 C. M. Dobson, *Nature*, 2003, **426**, 884.
- 2 D. Svozil, J. Kalina, M. Omelka and B. Schneider, *Nucleic Acids Res.*, 2008, **36**, 3690.
- 3 D. Djuranovic and B. Hartmann, *J. Biomol. Struct. Dyn.*, 2003, **20**, 771.
- 4 G. M. Clore, *J. Biomol. NMR*, 2011, **51**, 209.
- 5 A. I. Karsisiotis, N. M. Hessari, E. Novellino, G. P. Spada, A. Randazzo and M. Webba da Silva, *Angew. Chem., Int. Ed.*, 2011, **50**, 10645.
- 6 G. Papadakis, A. Tsortos, F. Bender, E. E. Ferapontova and E. Gizeli, *Anal. Chem.*, 2012, **84**, 1854.
- 7 S. Chatterjee, J. B. Lee, N. V. Valappil, D. Luo and V. M. Menon, *Nanoscale*, 2012, **4**, 1568.
- 8 Y. W. Cao, R. Jin and C. A. Mirkin, *Science*, 2002, **297**, 1536.
- 9 N. L. Rosi and C. A. Mirkin, *Chem. Rev.*, 2005, **105**, 1547.
- 10 J. Liu, Z. Cao and Y. Lu, *Chem. Rev.*, 2009, **109**, 1948.
- 11 D. Li, S. Song and C. Fan, *Acc. Chem. Res.*, 2010, **43**, 631.
- 12 Y. Song, W. Wei and X. Qu, *Adv. Mater.*, 2011, **23**, 4215.
- 13 F. Xia, X. Zuo, R. Yang, Y. Xiao, D. Kang, A. Vallée-Bélisle, X. Gong, J. D. Yuen, B. Y. Hsu, A. J. Heeger and K. W. Plaxco, *Proc. Natl. Acad. Sci. U. S. A.*, 2010, **107**, 10837.
- 14 J. Y. Kim and J. S. Lee, *Nano Lett.*, 2009, **9**, 4564.
- 15 S. Guo and E. Wang, *Acc. Chem. Res.*, 2011, **44**, 491.
- 16 X. Xue, F. Wang and X. Liu, *J. Mater. Chem.*, 2011, **21**, 13107.
- 17 J. Liu and Y. Lu, *J. Am. Chem. Soc.*, 2003, **125**, 6642.
- 18 M. Hong, X. Zhou, Z. Lu and J. Zhu, *Angew. Chem., Int. Ed.*, 2009, **48**, 9503.
- 19 K. Jang, H. Lee, H. Jin, Y. Park and J. Nam, *Small*, 2009, **5**, 2665.
- 20 P. Chen, D. Pan, C. Fan, J. Chen, K. Huang, D. Wang, H. Zhang, Y. Li, G. Feng, P. Liang, L. He and Y. Shi, *Nat. Nanotechnol.*, 2011, **6**, 639.
- 21 Y. Xiao, K. Y. Dane, T. Uzawa, A. Csordas, J. Qian, H. T. Soh, P. S. Daugherty, E. T. Lagally, A. J. Heeger and K. W. Plaxco, *J. Am. Chem. Soc.*, 2010, **132**, 15299.
- 22 M. M. Ali, P. Kanda, S. D. Aguirre and Y. Li, *Chem. – Eur. J.*, 2011, **17**, 2052.
- 23 X. Xie, W. Xu, T. Li and X. Liu, *Small*, 2011, **7**, 1393.
- 24 Y. Song, X. Xu, K. W. MacRenaris, X. Zhang, C. A. Mirkin and T. J. Meade, *Angew. Chem., Int. Ed.*, 2009, **48**, 9143.
- 25 H. Wang, W. Xu, H. Zhang, D. Li, Z. Yang, X. Xie, T. Li and X. Liu, *Small*, 2011, **7**, 1987.
- 26 J. Zhang, L. Wang, H. Zhang, F. Boey, S. Song and C. Fan, *Small*, 2010, **6**, 201.
- 27 A. E. Prigodich, O. S. Lee, W. L. Daniel, D. S. Seferos, G. C. Schatz and C. A. Mirkin, *J. Am. Chem. Soc.*, 2010, **132**, 10638.
- 28 Y. Huang, H. Liu, X. Xiong, Y. Chen and W. Tan, *J. Am. Chem. Soc.*, 2009, **131**, 17328.
- 29 X. Xue, W. Xu, F. Wang and X. Liu, *J. Am. Chem. Soc.*, 2009, **131**, 11668.
- 30 Z. Zhu, C. Wu, H. Liu, Y. Zou, X. Zhang, H. Kang, C. Yang and W. Tan, *Angew. Chem., Int. Ed.*, 2010, **49**, 1052.
- 31 X. Xue, F. Wang and X. Liu, *J. Am. Chem. Soc.*, 2008, **130**, 3244.
- 32 Y. Xiang and Y. Lu, *Nat. Chem.*, 2011, **3**, 697.
- 33 H. Wei, Z. Wang, J. Zhang, S. House, Y. Gao, L. Yang, H. Robinson, L. H. Tan, H. Xing, C. Hou, I. M. Robertson, J. Zuo and Y. Lu, *Nat. Nanotechnol.*, 2011, **6**, 93.
- 34 X. Xie, W. Xu and X. Liu, *Acc. Chem. Res.*, 2012, **45**, 1511.
- 35 J. Wang and X. Qu, *Nanoscale*, 2013, **5**, 3589.
- 36 W. Xu, X. Xie, D. Li, Z. Yang, T. Li and X. Liu, *Small*, 2012, **8**, 12.
- 37 E. Hutter and J. H. Fendler, *Adv. Mater.*, 2004, **16**, 1685.
- 38 J. Zhao, X. Zhang, C. R. Yonzon, A. J. Haes and R. P. Van Duyne, *Nanomedicine*, 2006, **1**, 219.
- 39 K. M. Mayer and J. H. Hafner, *Chem. Rev.*, 2011, **111**, 3828.
- 40 N. J. Halas, S. Lal, W.-S. Chang, S. Link and P. Nordlander, *Chem. Rev.*, 2011, **111**, 3913.
- 41 W. P. Hall, J. N. Anker, Y. Lin, J. Modica, M. Mrksich and R. P. Van Duyne, *J. Am. Chem. Soc.*, 2008, **130**, 5836.
- 42 A. J. Haes and R. P. Van Duyne, *J. Am. Chem. Soc.*, 2002, **124**, 10596.

- 43 J. Spadavecchia, A. Barras, J. Lyskawa, P. Woisel, W. Laure, C.-M. Pradier, R. Boukherroub and S. Szunerits, *Anal. Chem.*, 2013, **85**, 3288.
- 44 W. K. Choi, T. H. Liew, M. K. Dawood, H. I. Smith, C. V. Thompson and M. H. Hong, *Nano Lett.*, 2008, **8**, 3799.
- 45 J. Henzie, J. Lee, M. H. Lee, W. Hasan and T. W. Odom, *Annu. Rev. Phys. Chem.*, 2009, **60**, 147.
- 46 S. Cataldo, J. Zhao, F. Neubrech, B. Frank, C. Zhang, P. V. Braun and H. Giessen, *ACS Nano*, 2011, **6**, 979.
- 47 M. Rahmani, B. Lukyanchuk and M. Hong, *Laser Photonics Rev.*, 2013, **7**, 329.
- 48 H. Chen, X. Kou, Z. Yang, W. Ni and J. Wang, *Langmuir*, 2008, **24**, 5233.
- 49 P. R. West, S. Ishii, G. V. Naik, N. K. Emani, V. M. Shalaev and A. Boltasseva, *Laser Photonics Rev.*, 2010, **4**, 795.
- 50 J. A. Rice and D. M. Crothers, *Biochemistry*, 1989, **28**, 4512.
- 51 F. Stühmeier, A. Hillisch, R. M. Clegg and S. Diekmann, *J. Mol. Biol.*, 2000, **302**, 1081.
- 52 K. C. Grabar, R. G. Freeman, M. B. Hommer and M. J. Natan, *Anal. Chem.*, 1995, **67**, 735.
- 53 J. J. Storhoff, R. Elghanian, R. C. Mucic, C. A. Mirkin and R. L. Letsinger, *J. Am. Chem. Soc.*, 1998, **120**, 1959.